Latency-Constrained Fading Mitigation for Coherent Optical Feeder Links based on Space-Time-Frequency Coding

Korevaar, C. Willem; Saathof, Rudolf; van Abkoude, Tara; Doelman, Niek J.

DOI
10.1117/12.2690891

Publication date
2023

Document Version
Final published version

Published in
International Conference on Space Optics, ICSO 2022

PROCEEDINGS OF SPIE

SPIEDigitalLibrary.org/conference-proceedings-of-spie

Latency-constrained fading mitigation for coherent optical feeder links based on space-time-frequency coding

C. Willem Korevaar, Rudolf Saathof, Tara van Abkoude, Niek Doelman

C. Willem Korevaar, Rudolf Saathof, Tara van Abkoude, Niek Doelman, "Latency-constrained fading mitigation for coherent optical feeder links based on space-time-frequency coding," Proc. SPIE 12777, International Conference on Space Optics — ICSO 2022, 127774T (12 July 2023); doi: 10.1117/12.2690891

SPIE.

Event: International Conference on Space Optics — ICSO 2022, 2022, Dubrovnik, Croatia

International Conference on Space Optics—ICSO 2022

Dubrovnik, Croatia

3–7 October 2022

Edited by Kyriaki Minoglou, Nikos Karafolas, and Bruno Cugny,

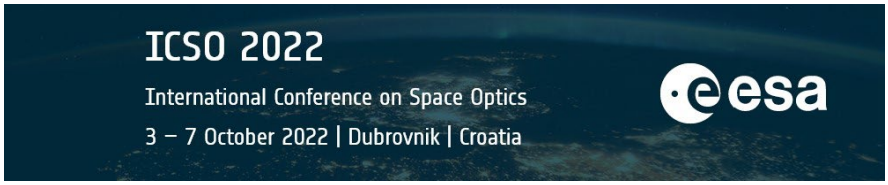

Latency-Constrained Fading Mitigation for Coherent Optical Feeder Links based on Space-Time-Frequency Coding

International Conference on Space Optics — ICSO 2022, edited by Kyriaki Minoglou, Nikos Karafolas, Bruno Cugny, Proc. of SPIE Vol. 12777, 127774T · © 2023 ESA and CNES · 0277-786X · doi: 10.1117/12.2690891

Latency-Constrained Fading Mitigation for Coherent Optical Feeder Links based on Space-Time-Frequency Coding

C. Willem Korevaar*[a], Rudolf Saathof[b], Tara van Abkoude[a], and Niek J. Doelman[a,c]

[a] Netherlands Organisation for Applied Research (TNO), Delft, The Netherlands
[b] Delft University of Technology, Delft, The Netherlands
[c] Leiden University, Leiden, The Netherlands

ABSTRACT

Optical feeder links (OFLs) benefit from the vast amount of bandwidth available in the THz-regime of the electromagnetic spectrum, and can be considered as enablers for future terabit-per-second satellite systems. A particular challenge for OFLs is to mitigate the effects of fading, caused by a combination of turbulence-induced scintillation, beam wander and pointing errors. The conventional solution is to exploit temporal diversity by a combination of interleaving and forward error correction (FEC). In this study we present an overview of fading mitigation techniques for latency-constrained coherent ground-to-satellite OFL and contribute a generic model which combines various diversity schemes including temporal, spatial, frequency and site diversity. To unlock spatial diversity, multi-beam space-time block coding and multi-beam, multi-λ are proposed and simulated. Though space-time block coding (STBC) provides more diversity gain, it requires accurate timing synchronization at the transmitter and channel state information at the receiver. Temporal, frequency and site diversity all rely on some form of interleaving and the potential diversity, pros and cons of each of these diversity techniques are covered in the presented study. In general, with a strict latency constraint and a tight link budget, frequency diversity, spatial diversity – either by STBC or multi-beam multi-λ – and site diversity can be effective methods to mitigate the effects of fading and close the link budget.

Keywords: Optical feeder links, ground-to-satellite, free space optics, turbulence, fading, diversity, space-time block coding, spatial diversity.

1. INTRODUCTION

The next generation of telecommunication satellites and constellations will be characterized by ever-increasing datarates, to serve more and more end-users, offload data-intensive instruments and satisfy data-hungry applications. As we enter the terabit-per-second regime, we face problems with conventional radio frequency (RF) feeder links as they require either very large numbers of ground gateways, which drives up the costs of the ground segment, or unrealistically high signal-to-noise ratios (SNRs). A promising alternative is found in optical feeder links (OFLs),[1] which benefit from the vast amount of bandwidth available in the THz regime of the electromagnetic spectrum, and could enable license- and interference-free terabit-per-second satellite connections.

A particular challenge for OFLs is to mitigate the effects of fading, caused by a combination of turbulence-induced scintillation, beam wander and pointing errors. These effects cause random fluctuations of the received intensity and phase.[2] As a result the receive power, and thereby the SNR and bit error rate (BER) become time-dependent and due to fades there can be large bursts of bit errors. The conventional solution is to overcome these by temporal diversity, e.g., a combination of temporal (channel) interleaving and forward error correction (FEC).[3] However, as the coherence time of the ground-to-satellite link is typically in the order of milliseconds, long interleavers of up to hundreds of milliseconds are required. This leads to high latency, on top of the earth-to-satellite round-trip time, which is unacceptable for many end-user applications. In this paper we present and discuss alternatives which can be deployed to mitigate fading while constraining the additive latency.

* E-mail: wim.korevaar@tno.nl

Spatial diversity has been studied extensively, in particular for RF applications, optical satellite-to-ground links and links employing direct detection. For optical satellite-to-ground links aperture averaging and adaptive optics are widely applied to average out and correct wavefront distortions.[4,5] However, for ground-to-satellite links the receiver can be modelled as a point receiver which means that there is essentially nothing to average or correct, and thereby no diversity gain to be booked. Techniques like transmit beam pre-compensation or adaptive power control may work, but require that the point ahead angle (PAA) is smaller than the isoplanatic angle to guarantee that the channel state information is sufficiently accurate, which is typically not the case for low Earth orbit (LEO) and debatable for geostationary orbit (GEO). Transmitter diversity for direct detection systems has been demonstrated by experimental systems to be an effective method[6–8] and is based on the superposition principle of incoherent transmit beams, whereby each of the beams is affected by uncorrelated wavefront distortions. This principle can not be used for coherent systems, as the phase information would be lost due to incoherent combining of multiple beams at the receiver aperture. This leaves us with the question which diversity methods can be fruitfully applied for ground-to-satellite links employing coherent optics, with a latency constraint. This question forms the main rationale behind the presented research.

The rest of the paper is organized as follows: Section 2 describes the transmitter, channel and receiver model and explains the benefits of coherent detection in the context of fading mitigation. It provides a generic model which allows for combined temporal, frequency, spatial and site diversity. Section 3 elaborates on the diversity techniques and coherence metrics and details how we can exploit diversity along the dimensions of space-time-frequency. In particular space-time block coding (STBC) and a technique which we call multi-beam, multi-λ are more extensively discussed. A ground-to-satellite link is simulated, under moderate turbulence conditions, and the results are presented in Section 4, which provides comparative results for the (combined) diversity techniques. Finally, Section 5 concludes this paper, presents a discussion of the results and directions for further research.

2. SYSTEM & CHANNEL MODEL

2.1 Transmitter

We consider a generic description of a multi-channel ground-to-satellite link which employs temporal, frequency, spatial and site diversity. The transmitter performs error correction coding of an input bitstream and interleaves the resulting FEC symbols in time. The resulting bitstream is mapped to symbols, which are drawn from a (complex) signal constellation, to form a sequence $\mathbf{s}$. Each symbol $s_{\{\dots\}}$, being an element of $\mathbf{s}$, is chosen in correspondence with a generator matrix $G(n,k,o)$ as described in Section 3. The symbol $s_{\{\dots\}}$ is mapped to a time slot n, carrier frequency $f_0 + k\Delta f$, transmit beam b and ground station o, with zero-based indexing. In a generalized way, this can be described by a transmit signal:

$$x_{o,b}(t) \triangleq \mathrm{Re}\left\{ \sqrt{\frac{2P_t}{B \cdot K}} \sum_{n=0}^{\infty} \sum_{k=0}^{K-1} s_{\{\mathrm{mod}(n,B),b\}} \cdot g(t - nT_s) \cdot e^{j2\pi((f_0 + k\Delta f)t + \phi_k(t))} \right\}, \tag{1}$$

where B denotes the number of transmit beams (per OFL), K the number of optical channels, Δf the channel spacing in frequency, f_0 the carrier frequency of the first optical channel, $\phi_k(t)$ represents the combined initial laser offset and phase noise, P_t the total transmit power (per OFL), $\mathrm{mod}(\cdot,\cdot)$ the modulus operation and $g(t)$ the prototype waveform used for pulseshaping. We assume $g(t)$ to be a non-return-to-zero (NRZ) rectangular function with a symbol duration T_s.

2.2 Channel

After propagation through the (turbulent) channel, the received signal at the o^{th} telescope of the satellite can be described by the sum of the B simultaneously received, spatially overlapping transmit beams $x_{o,b}(t)$:

$$r_o(t) = \sum_{b=0}^{B-1} h_{o,b}(t) \cdot x_{o,b}(t) + n_{o,b}(t), \tag{2}$$

with $h_{o,b}(t)$ and $n_{o,b}(t)$ being the complex channel coefficient and (background) noise term for the o^{th} optical ground station (OGS) and b^{th} transmit beam, respectively. The complex channel coefficient can be decomposed in a channel gain which equals $|h_{o,b}| = \sqrt{L_o \cdot I_{o,b}}$ and a complex phase factor $\mathrm{e}^{j\mathrm{Arg}(h_{o,b})}$. The phase fluctuations are assumed to be uniformly distributed over the interval $[0, 2\pi)$. L_o is the aggregate static link loss of OFL o which is the product of transmitter and receiver efficiencies, optical amplification stages, telescope gains and free-space path losses. The irradiance fluctuations of each channel $I_{o,b}$, for turbulence regimes varying from weak to strong, can be accurately modelled by the Gamma-Gamma distribution:[2]

$$p\left(I_{o,b}\right) = 2\frac{(\alpha\beta)^{(\alpha+\beta)/2}}{\Gamma(\alpha)\Gamma(\beta)} I_{o,b}^{(\alpha+\beta)/2-1} \mathrm{K}_{\alpha-\beta}\left(2\sqrt{\alpha\beta I_{o,b}}\right) \qquad \text{for } I_{o,b} > 0, \alpha > 0, \beta > 0, \tag{3}$$

where $\Gamma(\cdot)$ and $\mathrm{K}_p(\cdot)$ are the Gamma function and modified Bessel function of the second kind of order p, respectively. The characteristic parameters α and β model the small- and large-scale scintillations and are coupled to the scintillation index by $\sigma_I^2 = 1/\alpha + 1/\beta + 1/(\alpha\beta)$. Though one could model the fluctuations due to beam wander and pointing errors as well,[9] we restrict ourselves to (3) since our primary interest is in diversity techniques rather than the irradiance models.

As this study aims to overcome the irradiance fluctuations by temporal, frequency and spatial diversity it is important to understand the channel's coherence time T_c, coherence bandwidth Ω_c and coherence distance Z_c. If the time difference, frequency difference and/or spatial separation between two transmitted FEC symbols is sufficiently large, then we can assume that those symbols are affected by a channel response $h_{o,b}$ which is independent (and identically distributed) and exploit diversity. These coherence metrics are discussed in Section 3 which covers the topic of diversity.

Note, the channel can be characterized as block and flat fading channel as the coherence time T_c and coherence bandwidth Ω_c are considerably larger than the symbol time and channel bandwidth, respectively. Therefore, the channel coefficients $h_{o,b}$ can be considered to be a complex constant over a number of symbol periods for each optical channel. Consequently, accurate channel state information can be obtained at the receiver, through estimating the channel coefficients with training symbols.

2.3 Receiver

At the receiver, the received signal is demultiplexed into the distinct optical channels. Each channel is then fed to a 3 dB-splitter and a 180°-hybrid to feed the sum and difference terms of the electric fields of the receive signal E_r and the local oscillator (LO) E_{LO} to a balanced detector with a matched filter. The electric field of the LO is described by $E_{\text{LO}} = \sqrt{P_{\text{LO}}} e^{j(2\pi f_{\text{LO}} t + \phi_{\text{LO}}(t))}$ with P_{LO}, f_{LO} and $\phi_{\text{LO}}(t)$ being the power, frequency and phase (noise) term of the LO, respectively. The resulting photo current, while excluding noise terms for the sake of clarity, for the k^{th} optical channel of OFL o becomes:

$$\begin{aligned}
\hat{i}_{o,k}(t) &= \frac{R_d}{2}\left(|E_r + E_{\text{LO}}|^2 - |E_r - E_{\text{LO}}|^2\right) \\
&= 2R_d\sqrt{\frac{2P_t P_{\text{LO}}}{B \cdot K}} \cdot \sum_{b=0}^{B-1} h_{o,b}(t) \cdot s_{\{\ldots\}} \cdot \cos\left(2\pi(f_0 + k\Delta f - f_{\text{LO}}) + \phi_k(t) - \phi_{\text{LO}}(t)\right) \text{with } -T_s/2 \le t < T_s/2 \\
&= 2R_d\sqrt{\frac{2P_t P_{\text{LO}}}{B \cdot K}} \cdot \sum_{b=0}^{B-1} h_{o,b}(t) \cdot s_{\{\ldots\}} \qquad \text{with } f_{\text{LO}} = f_0 + k\Delta f,\ \phi_{\text{LO}}(t) = \phi_k(t),
\end{aligned} \tag{4}$$

where R_d is the responsivity of the photodetector and homodyne detection is assumed such that $f_{\text{LO}} = f_0 + k\Delta f$ with a phase locked loop, i.e., $\phi_{\text{LO}}(t) = \phi_k(t)$. Our received photo current is affected by several noise mechanisms which include beat terms of both signal and input noise with the LO, shot noise, intensity noise, phase noise and thermal noise. One of the advantages of the coherent receiver is that we can use a high LO power and thereby

operate in the shot-noise limited regime and assume the other noise contributions negligible. As the shot noise is dominated by the part associated with the LO power, which is typically large in contrast to the receive signal, we can approximate it as an additive white Gaussian noise (AWGN) source.

A clear advantage of coherent detection is that the photo-current in (4) is dependent on $h_{\{\ldots\}}$ rather than $h^2_{\{\ldots\}}$ as in thermal-noise limited direct-detection systems. This means that the SNR is proportional to the receive power $P_r(t)$ (rather than $P_r^2(t)$). As a consequence, the irradiance fluctuations lead to smaller SNR and BER degradations in the case of shot-noise limited coherent detection in comparison to thermal-noised limited direct detection. This helps to meet our goal of fading mitigation and limit the required temporal interleaving depth and its associated latency.

3. ANALYSIS - DIVERSITY METHODS

Ideally, we could realize full diversity among the dimensions of time-frequency-space while achieving full-rate, low-latency communications and a low system complexity. In practice, the extent to which we succeed in exploiting temporal, frequency and spatial diversity depends on the diversity which we can realize in the respective domains.

3.1 Temporal diversity

The coherence time for clear sky and strong turbulence conditions is typically in the order of 0.1-10 ms.[3] A measurement campaign for GEO ground-to-satellite optical links has shown that some fades have durations up to 100 ms.[10] In order to exploit temporal diversity we need to assure that (some of) the symbols are separated in time with a temporal separation larger than the coherence time such that the channel coefficients become independent. A mapping function is used $\pi_T(\cdot)$ such that an interleaved symbol vector $\tilde{\mathbf{c}}$ is created based on the FEC symbol vector $\mathbf{c}$ such that $\tilde{c}_i = c_{\pi_T(i)}$ where i is the index of the interleaved symbol vector. By applying an interleaver we essentially spread out the impact of fades over multiple code blocks such that – with sufficient error correction capability – the distributed errors can be handled by the error correction algorithm. With a latency constraint of L for the interleaver and a coherence time of T_c, we can get about L/T_c independent transmissions during a block code.

3.2 Frequency diversity

The ground-to-satellite path is typically characterized by a very short impulse response with hardly any delay spread and negligible inter-symbol interference (ISI). The coherence bandwidth – being the inverse of the RMS delay spread of the channel – is typically in the order of 1-100 THz.[11] However, when there is rain, fog or thin (cirrus) clouds – due to scattering – the delay spread increases and the coherence bandwidth can drop to 100 GHz.[12] Assuming a multi-channel OFL the transfer function for optical channels which are spaced at $\Delta f > \Omega_c$ could be regarded as independent (but identically distributed) which provides additional diversity. To exploit frequency diversity we can interleave FEC symbols in a similar way to conventional temporal interleaving. A mapping function $\pi_\Omega(\cdot)$ interleaves symbols from the FEC symbol vector $\mathbf{c}$ to form a new vector $\tilde{\mathbf{c}}$, with $\tilde{c}_i = c_{\pi_\Omega(i)}$. The aim is to maximize the distance between input FEC symbols, not just in time, but in time-frequency. With a complete bandwidth Ω (e.g., 4.8 THz for the infrared C-band) and a coherence bandwidth of Ω_c we can theoretically get Ω/Ω_c independent transmissions, at the same time instant. Frequency diversity may be very welcome when there is additional loss due to thin clouds, provided that the losses do not become too high to close the link budget.

3.3 Spatial diversity

In addition to the temporal and frequency domain, the spatial domain can be considered for additional diversity. While for an uplink path, the spatial coherence distance at the satellite is many times larger than the probable size of the satellite, the coherence distances, at sea level, is roughly 2–30 cm at visible and IR wavelengths.[13] Given the large receive apertures, and small transmit beam waist typically used, one can fit multiple transmit beams in the receive aperture,[14] create multiple independent (but identically distributed) transmit channels provided that the spatial separation, i.e., $\sqrt{\Delta x^2 + \Delta y^2}$, between two transmit beams is larger than the coherence distance

Z_c. Given the large coherence distance at the satellite, multiple receivers at the satellite will essentially measure the same signal, and not provide additional diversity. Consequently, a multiple-input single-output (MISO) configuration with B transmit beams and a single receiver, is the configuration of interest to attain spatial diversity gain.

3.3.1 Space-time block coding

Alamouti has proposed a very simple and elegant scheme for 2×1 MISO systems to exploit transmit diversity. It is characterized by maximum diversity gain, full-rate transmission, maximum-likelihood linear decoding and does not require channel state information at the transmitting end (only at the receiver).[15] Considering a transmitter employing the Alamouti scheme, the symbols $s_{\{\alpha,\beta\}}$ as in (1) are chosen in correspondence to the α^{th} row and β^{th} column, with zero-based indexing, of the STBC generator matrix $G_{2\times2}(n,k,o)$:

$$G_{2\times2}(n,k,o) \triangleq \begin{bmatrix} x_\eta & x_{\eta+1} \\ -x^*_{\eta+1} & x^*_\eta \end{bmatrix} \qquad \text{with}\, \eta \triangleq ((\lfloor n/B \rfloor O + o)\, K + k)\, B, \tag{5}$$

with $(\cdot)^*$ representing complex conjugation and $\lfloor\cdot\rfloor$ the floor function. The formulation for η allows for STBC in combination with interleaving of the symbols over K optical channels and O OGS sites. A visualization of the interleaving is shown in Table 1.

Unfortunately, there is not a natural extension from the Alamouti scheme to $N\times1$ MISO configurations. E.g., it can be proven that there does not exist a full-rate, orthogonal STBC for four transmit beams which achieves full diversity. This leaves us with the choice to either relax the full-rate, the orthogonality or the full diversity constraint. As we usually not operate under very high SNR conditions, we relax the orthogonality constraint at the cost of a small noise penalty, and can create a rotated quasi-orthogonal STBC by $[G_{2\times2}(n,k,o), \tilde{G}_{2\times2}(n+2,k,o); -\tilde{G}^*_{2\times2}(n+2,k,o), G^*_{2\times2}(n,k,o)]$:[16]

$$G_{4\times4}(n,k,o) \triangleq \begin{bmatrix} x_\eta & x_{\eta+1} & \tilde{x}_{\eta+2} & \tilde{x}_{\eta+3} \\ -x^*_{\eta+1} & x^*_\eta & -\tilde{x}^*_{\eta+3} & \tilde{x}^*_{\eta+2} \\ -\tilde{x}^*_{\eta+2} & -\tilde{x}^*_{\eta+3} & x^*_\eta & x^*_{\eta+1} \\ \tilde{x}_{\eta+3} & -\tilde{x}_{\eta+2} & -x_{\eta+1} & x_\eta \end{bmatrix} \qquad \text{with}\, \eta \triangleq ((\lfloor n/B \rfloor O + o)\, K + k)\, B, \tag{6}$$

where a rotated constellation is used with $\tilde{x} = x \cdot \mathrm{e}^{j\pi/4}$, to assure that a full diversity order of 4 is achieved.[16] The maximum-likelihood decoding follows a pairwise minimization as described in.[16] Note that decoding assumes channel state information at the receiver and accurate synchronization among the different transmit beams. If one of these conditions is not met, then the performance may be severely degraded.

Description	Dimensions	Param	Index of interleaved sequence
Symbols			0 0 1 1 2 2 3 3 4 4 5 5 6 6 7 7 8 8 9 9 10 10 11 11 12 ..
Time slots N	∞	n	0 1 0 1 0 1 0 1 0 1 0 1 0 1 0 1 0 1 0 1 0 1 0 1 2 ..
Transmit beams B	2	b	0 1 1 0 0 1 1 0 0 1 1 0 0 1 1 0 0 1 1 0 0 1 1 0 0 ..
Channels K	3	k	0 0 0 0 1 1 1 1 2 2 2 2 0 0 0 0 1 1 1 1 2 2 2 2 0 ..
Sites O	2	o	0 0 0 0 0 0 0 0 0 0 0 0 1 1 1 1 1 1 1 1 1 1 1 1 0 ..

Table 1. Visualization of the process of interleaving symbols over the dimensions of time, space, frequency and OFLs sites. This example illustrates a transmitter following the model in (1) employing the STBC generator matrix of (5), and uses arbitrary values $\{N,B,K,O\}$ for illustrative purposes. The indices of the symbols $s \in \mathbf{s}$ are shown in the top row of the table with directly underneath the tuples $\{n,b,k,o\}$ which shows the mapping of the symbol to the specified time, transmit beam, frequency and OFL indices.

3.3.2 Multi-beam, multi-λ

Dependent on the system configuration, it may not always be possible to meet the requirements for STBC, i.e., accurate timing synchronization and channel state information. As wavelength multiplexing is envisioned to be used for high-throughput OFLs,[14] an alternative is proposed; to assign each transmit beam to a distinct wavelength. The symbols $s_{\{\alpha,\beta\}}$ are chosen in correspondence to the α^{th} row and β^{th} column, with zero-based indexing, of the generator matrix $\Lambda_{2\times2}(n,k,o)$:

$$\Lambda_{2\times2}(n,k,o) \triangleq \begin{bmatrix} x_{\eta} & x_{\eta+1}\cdot \mathrm{e}^{j2\pi\Delta\Omega} \\ x_{\eta+2} & x_{\eta+3}\cdot \mathrm{e}^{j2\pi\Delta\Omega} \end{bmatrix} \qquad \text{with } \eta \triangleq \left(\left(\lfloor n/B^2 \rfloor O + o\right) K + k\right) B^2, \quad (7)$$

where $\Delta\Omega$ resembles the frequency separation required to demultiplex the two signals. The choice of $\Delta\Omega$ is dependent on the baudrate, prototype waveform $g(t)$ and (matched) filter capabilities. Note that it is important that the choice of $\Delta\Omega$ does not lead any of the transmit beams to spectrally overlap with any of the other K optical channels, all to avoid inter-channel interference. The matrix in (8) is easily extended to a 4×4 configuration:

$$\Lambda_{4\times4}(n,k,o) \triangleq \begin{bmatrix} x_{\eta} & x_{\eta+1}\cdot \mathrm{e}^{j2\pi\cdot1\Delta\Omega} & x_{\eta+2}\cdot \mathrm{e}^{j2\pi\cdot2\Delta\Omega} & x_{\eta+3}\cdot \mathrm{e}^{j2\pi\cdot3\Delta\Omega} \\ x_{\eta+4} & x_{\eta+5}\cdot \mathrm{e}^{j2\pi\cdot1\Delta\Omega} & x_{\eta+6}\cdot \mathrm{e}^{j2\pi\cdot2\Delta\Omega} & x_{\eta+7}\cdot \mathrm{e}^{j2\pi\cdot3\Delta\Omega} \\ x_{\eta+8} & x_{\eta+9}\cdot \mathrm{e}^{j2\pi\cdot1\Delta\Omega} & x_{\eta+10}\cdot \mathrm{e}^{j2\pi\cdot2\Delta\Omega} & x_{\eta+11}\cdot \mathrm{e}^{j2\pi\cdot3\Delta\Omega} \\ x_{\eta+12} & x_{\eta+13}\cdot \mathrm{e}^{j2\pi\cdot1\Delta\Omega} & x_{\eta+14}\cdot \mathrm{e}^{j2\pi\cdot2\Delta\Omega} & x_{\eta+15}\cdot \mathrm{e}^{j2\pi\cdot3\Delta\Omega} \end{bmatrix}$$
$$\text{with } \eta \triangleq \left(\left(\lfloor n/B^2 \rfloor O + o\right) K + k\right) B^2. \quad (8)$$

We could get the impression that the multi-λ, multi-beam operates at B times the rate of the STBC scheme. However, we need to be aware that also B times as many optical (sub)channels are used. Effectively, both schemes are able to operate at a full rate per single wavelength channel, and it depends on the required diversity gain, wavelength plan and other system constraints which of the two schemes is preferred. A visualization of both STBC and multi-beam, multi-λ is shown in Fig. 1.

3.4 Site diversity - Multiple OFLs

As a single OFL is characterized by a low availability due to blockages like clouds, it is foreseen that multiple OGSs may connect – directly or by relaying – to a single telecommunication satellite. Multiple connections may be maintained and fuel the satellite with its data, simultaneously, requiring multiple receive telescopes at the satellite. Assuming O OFLs, each with independent fading, we can attain additional site diversity, which could be regarded as a corner case of spatial diversity. For simplicity reasons, we assume in this study that all the OFLs are characterized by identical (normalized) receive powers and fading statistics, though in practice geographically separated sites are likely to experience different link losses, weather and turbulence conditions. Site diversity could be achieved again by STBC, but would require very accurate timing synchronization among sites which is not easily accomplished. The proposed technique is to interleave the FEC symbols over several OFLs, similar to temporal or frequency interleaving. A mapping function is used $\pi_Z(\cdot)$ such that an interleaved symbol vector $\tilde{\mathbf{c}}$ is created based on the FEC symbol vector $\mathbf{c}$ such that $\tilde{c}_i = c_{\pi_Z(i)}$ where i is the index of the interleaved symbol vector. Note, it comes at the cost of inter-OGS routing latency and dependencies, which – dependent on the OGS locations and latency constraints – may or may not be acceptable.

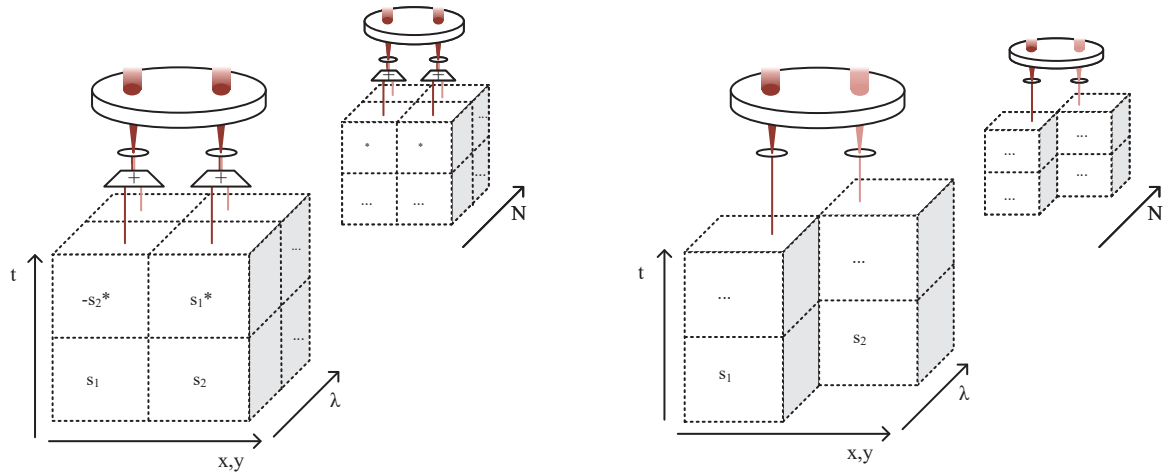

Figure 1. Visualization of multiplexing and diversity in the domains of time (t), frequency (λ), space (x, y) and OGS sites (N) for space-time block coding (*left*) and multi-beam, multi-λ (*right*). Both schemes transmit – with the time-frequency-space-site bins shown – a total of 8 (complex) symbols and the transmission of symbols s_1 and s_2 are highlighted.

3.5 On the outage capacities & probabilities

The multi-beam, multi-λ as well as the temporal, frequency and site diversity techniques all rely on some form of interleaving FEC symbols such that the FEC symbols are spread out in space-time-frequency. Consequently, the FEC symbols within a codeword are affected by multiple independent transmissions, which leads to D-fold diversity, with $D = O \cdot B \cdot F$ where O, B, F represent the number of independent optical feeder links, transmitter beams and frequency bands, respectively. Note, that D could include temporal interleaving as well, but is excluded to distinguish the temporal interleaving from the other diversity methods.

To assess the performance of the diversity techniques it is instructive to look at the outage probability, i.e., the probability that a certain desired spectral efficiency R (in bits/s/Hz) is not met by the channel capacity. For a slow fading channel – with coherence time T_c much larger than the symbol time and without interleaving – the outage probability is:

$$p_{\mathrm{OUT}}(R) \triangleq \mathbb{P}\left\{\log_2\left(1 + |h|^2\,\mathrm{SNR}\right) < R\right\} \tag{9}$$

whereby SNR is defined as the average receive signal energy divided by the average noise energy, $|h|^2\,\mathrm{SNR}$ resembles the instantaneous SNR and the outage probability is directly dependent on the channel coefficient h. We can considerably improve the outage probability by applying interleaving such that we get multiple independent transmissions. We essentially construct D parallel channels such that the outage probability becomes an average of all the achievable rates given D channel coefficients $h(\delta)$:

$$p_{\mathrm{OUT,ITL}}(R) \triangleq \mathbb{P}\left\{\frac{1}{D}\sum_{\delta=1}^{D}\log_2\left(1 + |h(\delta)|^2\,\mathrm{SNR}\right) < R\right\} \tag{10}$$

With the STBC decoders we do not average over independent channels, but receive B space-time coded beams in the decoder, all scaled in power by $1/B$. This leads to an outage probability of:[17]

$$p_{\mathrm{OUT,STBC}}(R) \triangleq \mathbb{P}\left\{\log_2\left(1 + \|\mathbf{h}\|^2\,\frac{\mathrm{SNR}}{B}\right) < R\right\} \tag{11}$$

with $\mathbf{h}$ being the vector with B channel coefficients. The two equations (10) and (11) allow us to compare the B-fold transmit diversity to the D-fold interleaving-based diversity. By Jensen's inequality for concave functions we know that:

$$\frac{1}{D}\sum_{\delta=1}^{D}\log_2\left(1+|h(\delta)|^2\,\mathrm{SNR}\right)\leq\log_2\left(1+\|\mathbf{h}\|^2\,\frac{\mathrm{SNR}}{B}\right) \tag{12}$$

which indicates that the achievable rate for STBC is always equal or higher than the rate for interleaving-based diversity techniques, assuming $B = D$. Equality is only met when the summands $\mathbf{h}$ are all equal, which is – by definition – not the case if we aim for spatial diversity. This will also be shown by simulations in Section 4. It should be said however that despite the better performance of STBC, it still suffers from an SNR penalty by $1/B$ as shown in (11). If we want to overcome this, then we need channel state information (CSI) also at the transmitter. With full CSI, we can pre-correct the transmit beams (e.g., with an extra phase shift or adaptive optics) to assure that the B beams constructively interfere at the receive aperture, and thereby minimize the outage probability:

$$p_{\mathrm{OUT,TX-CSI}}(R)\triangleq\mathbb{P}\left\{\log_2\left(1+\|\mathbf{h}\|^2\,\mathrm{SNR}\right)<R\right\}. \tag{13}$$

As explained in Section 1 accurate CSI at the transmitter may not be available. Therefore, we direct our attention in upcoming sections to diversity techniques requiring no CSI or CSI only at the receiver.

4. RESULTS

4.1 Simulation model

A ground-to-satellite OFL has been simulated using Mathworks MATLAB, based on the system and channel model sketched in Section 2. We have simulated fading based on a Gamma-Gamma distribution, with exponential covariance function, for moderate turbulence conditions with $\alpha = 4.0$ and $\beta = 1.9$ and $\tau_c = 0.01$ s. The parameter τ_c, related to the coherence time T_c, is defined by the time where the (normalized) exponential covariance function decayed to 1/e,[18] and the required length of the (temporal) interleaver is proportional to this parameter. The fading realizations of the channel model are generated based on the methodology in[18,19] and have a duration of 100 s and a sampling interval of 0.1 ms. Each simulation run simulates 400 000 frames, which are either uncoded or Reed-Solomon (n,k) coded, which is either (255,233) or (255,127), where n resembles the block length, k the message length and the coding rate is k/n. Interleaving takes place, not on symbols, but on the Reed-Solomon FEC symbols, as we prefer to have all potential bit errors in a single symbol rather than in multiple symbols. Maximum distance separable codes like Reed-Solomon offer optimal burst erasure protection, which is desired for block fading channels.[20] Note that by applying (multiple) diversity techniques, the nature of the error distribution changes from bursty to random, and other coding schemes may offer better performance.[21] All considered, for our OFL design we have chosen for Reed-Solomon coding as it strikes a good balance between coding gain, computational and power-efficiency, which is important as the envisioned datarates are in the order of terabit-per-second and the heavy lifting – the decoding – takes place on-board of the satellite.

4.2 Simulation results

The top-row plots of Fig. 2 show the BER for QPSK with STBC, for both additive white Gaussian noise (AWGN) and fading channel, with and without uniform interleaving of FEC symbols over a duration of 50 ms, employing RS(255,223) and RS(225,127), and with $B \in \{1, 2, 4\}$. No additional spatial, frequency or site diversity is employed. The combined coding and diversity gain without interleaver is 0.5 dB, 8.5 dB, 12.5 dB for 1, 2 and 4 transmitter configurations, for a BER of 1E-5, with RS(255,223). Lowering the coding rate, by using RS(255,127), gives 1.5, 9.5 and 14.5 dB gain, respectively. Though considerable diversity gain is achieved, adding an additional interleaver, constrained to 50 ms, can still provide additional dBs in diversity gain as is visible in the top-right plots of Fig. 2. With an interleaver constrained to 50 ms and RS(255,223), a coding

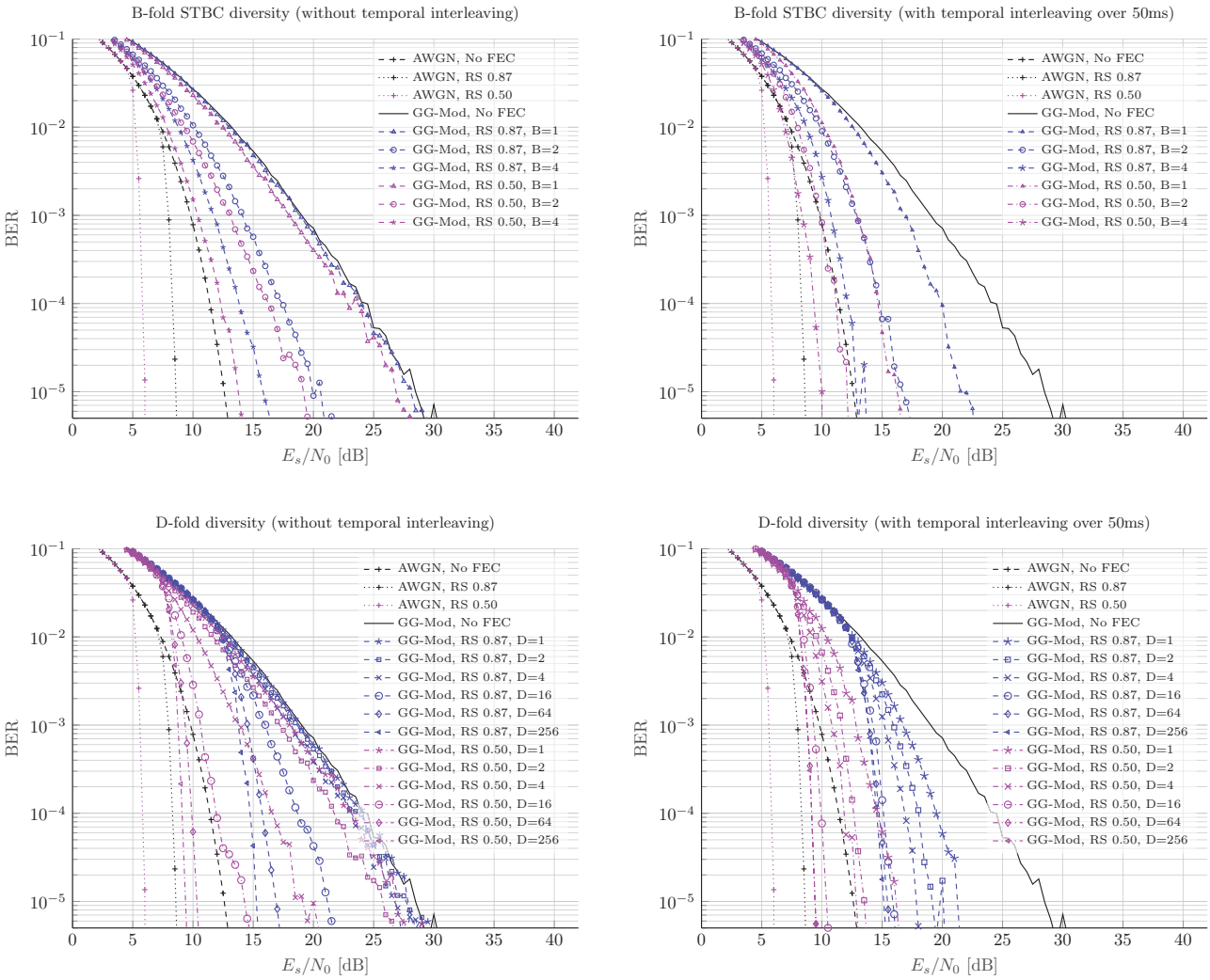

Figure 2. BER curves for OFL characterized by a Gamma-Gamma fading channel with moderate turbulence (and AWGN as a reference case). The top row plots show various MISO configurations employing STBC whereas the bottom row plots are without STBC, but with several values of the diversity parameter D which resembles the number of independent fading gains – due to frequency, spatial and/or site diversity – in each codeword. The applied coding is Reed-Solomon (255,223) and (255,127) with respective coding rates of 0.87 and 0.50, respectively.

and diversity gain of 6.5 dB, 13.5 dB, 15 dB is achieved, respectively. With RS(255,127) this becomes 12.5 dB, 16.5 dB, 18.5 dB, respectively.

The multi-beam, multi-λ as well as the temporal, frequency and site diversity techniques all rely on interleaving FEC symbols such that essentially D independent transmissions are created, whereby $D = O \cdot B \cdot F$ with O, B, F representing the number of optical feeder links, transmitter beams and frequency bands, respectively. The BER curves for different values of D are shown in the bottom plots of Fig. 2. As the block length is 256 FEC symbols, with $D = 256$ essentially all the FEC symbols undergo independent fading. Additional temporal interleaving then does not improve the BER curves. For smaller values of D, additional temporal diversity is beneficial and can provide additional dBs in diversity gain as is visible from the bottom-right plots in Fig. 2.

The error probabilities for the cases where $B = D$ show that (QO)-STBC clearly outperforms the interleaving-

based diversity techniques. This is in line with the analysis of the outage probabilities in Section 3.5. Note, that the differences are large for small B and D, but in the limit for large diversity orders with sufficiently high coding rates, become comparable. Though the plots show a limit set of combinations, it is important to stress that – as an example – STBC can also be combined with temporal, frequency and site diversity, as described by the generic transmit & diversity model in (1).

5. CONCLUSIONS

In this study we have presented the problem of latency-constrained fading mitigation for coherent optical ground-to-satellite links and have contributed a generic model which combines various diversity schemes including temporal, spatial, frequency and site diversity. We have elaborated on the typical coherence times, bandwidth and distances to assess how the dimensions of time-frequency-space can be exploited to book diversity gain.

It was shown that employing coherent detection in fading channels provides a large performance gain over thermal-noise limited direct detection schemes. This helps to meet our goal of fading mitigation and limit the required temporal interleaving depth and its associated latency. We have also discussed the outage capacities and probabilities for several diversity techniques and have shown the superiority of STBC. Dependent on the system configuration, it may not always be possible to meet the requirements for STBC, i.e., accurate timing synchronization and channel state information. As wavelength multiplexing is envisioned to be used for high-throughput OFLs, an alternative has been proposed by assigning distinct sets of wavelengths to different transmit beams. The FEC codewords are essentially split into B parts, modulated onto B different optical carriers and transmitted by B transmit beams. This leads to B-fold diversity. Both spatial diversity methods can be complemented by temporal, frequency and site diversity as shown in Sections 3 and 4.

Without a (stringent) latency constraint, we may mitigate the effects of fading by our usual suspects; temporal channel interleaving and FEC. However, if there is a strict latency constraint and more diversity gain is required, then STBC can unlock maximum diversity gain as long as the requirements of accurate timing synchronization among the transmitter beams and accurate channel state information at the receiver can be met. If that is not the case, then one can consider multi-beam, multi-λ transmission, which comes with a lower system complexity, but also provides less diversity gain. In case of multi-channel feeder links we can also – without much complexity – interleave the optical channels, which may provide additional diversity in case there are thin (cirrus) clouds. Under such circumstances, some extra dBs may be more than welcome, provided that we can still close the link budget. Finally, we have shown the possibility to extend the diversity schemes by multi-OFL diversity. Though this provides the same diversity gain as the other interleaving-based diversity techniques, it may be questionable whether the additional gains outweigh the additional complexity, latency and interdependencies. In general, the optimum (mix of) diversity techniques is dependent on the use-case, link budget, required diversity gain and system constraints. Though we researched several diversity techniques along many dimensions, even more combinations can be considered in follow-up studies. It may be of interest to study extensions to STBC like space-time-frequency block coding, and interleaving functions in time, frequency and space to provably maximize the distance between subsequent FEC symbols and thereby maximally exploit the channel diversity.

In conclusion, with a latency constraint, a single diversity method – like a temporal interleaver – may not provide sufficient diversity gain to close the link budget. We have proposed, discussed and shown the effectiveness of combinations of temporal, frequency, spatial and site diversity. All with the aim to mitigate the effects of fading and to pave the way for robust, high-throughput OFLs while keeping the latency within limits.

ACKNOWLEDGMENTS

This study has been conducted as part of the TNO Early Research Program “Laser Satellite Communication - High Throughput Optical Feeder Links”.

REFERENCES

[1] Kaushal, H. and Kaddoum, G., "Optical communication in space: Challenges and mitigation techniques," *IEEE Communications Surveys & Tutorials* **19**(1), 57–96 (2017).

[2] Al-Habash, A., Andrews, L. C., and Phillips, R. L., "Mathematical model for the irradiance probability density function of a laser beam propagating through turbulent media," *Optical engineering* **40**(8), 1554–1562 (2001).

[3] Khalighi, M. A. and Uysal, M., "Survey on free space optical communication: A communication theory perspective," *IEEE communications surveys & tutorials* **16**(4), 2231–2258 (2014).

[4] Khalighi, M.-A., Schwartz, N., Aitamer, N., and Bourennane, S., "Fading reduction by aperture averaging and spatial diversity in optical wireless systems," *Journal of optical communications and networking* **1**(6), 580–593 (2009).

[5] Saathof, R., Den Breeje, R., Klop, W., Kuiper, S., Doelman, N., Pettazzi, F., Vosteen, A., Truyens, N., Crowcombe, W., Human, J., et al., "Optical technologies for terabit/s-throughput feeder link," in [*Proc. IEEE International Conf. on Space Optical Systems and Applications*], 123–129 (2017).

[6] Jeganathan, M., Toyoshima, M., Wilson, K. E., James, J. C., Xu, G., and Lesh, J. R., "Data analysis results from the gold experiments," in [*Free-Space Laser Communication Technologies IX*], **2990**, 70–81, SPIE (1997).

[7] Caplan, D., Carney, J., Lafon, R., and Stevens, M., "Design of a 40-watt 1.55 μm uplink transmitter for lunar laser communications," in [*Free-Space Laser Communication Technologies XXIV*], **8246**, 144–152, SPIE (2012).

[8] Calvo, R. M., Becker, P., Giggenbach, D., Moll, F., Schwarzer, M., Hinz, M., and Sodnik, Z., "Transmitter diversity verification on artemis geostationary satellite," in [*Free-Space Laser Communication and Atmospheric Propagation XXVI*], **8971**, 24–37, SPIE (2014).

[9] Sandalidis, H. G., Tsiftsis, T., and Karagiannidis, G. K., "Optical wireless communications with heterodyne detection over turbulence channels with pointing errors," *J. Lightwave Technol.* **27**, 4440–4445 (Oct 2009).

[10] Saucke, K., Mahn, R., Pimentel, P. M., Heine, F., Mata-Calvo, R., Surof, J., Barrios, R., Reeves, A., Bischl, H., Brandt, H., et al., "Three years of optical satellite to ground links with the t-aogs: data transmission and characterization of atmospheric conditions," in [*International Conference on Space Optics—ICSO 2018*], **11180**, 525–534, SPIE (2019).

[11] Kelly, D. E., Young, C. Y., and Andrews, L. C., "Temporal broadening of ultrashort space-time gaussian pulses with applications in laser satellite communication," in [*Free-Space Laser Communication Technologies X*], **3266**, 231–240, SPIE (1998).

[12] Grabner, M. and Kvicera, V., "Multiple scattering in rain and fog on free-space optical links," *J. Lightwave Technol.* **32**, 513–520 (Feb 2014).

[13] Andrews, L. C. and Phillips, R. L., "Laser beam propagation through random media," *Laser Beam Propagation Through Random Media: Second Edition* (2005).

[14] Silvestri, F., Pettazzi, F., Eschen, M., Boschma, J. J., Lutgerink, J. B., Kramer, G. F., Korevaar, C. W., den Breeje, R., Duque, C. M., and Doelman, N. J., "Beam multiplexing for satellite communication optical feeder links," in [*Proc. SPIE Free-Space Laser Communications XXXII*], 1–9 (2020).

[15] Alamouti, S. M., "A simple transmit diversity technique for wireless communications," *IEEE Journal on selected areas in communications* **16**(8), 1451–1458 (1998).

[16] Jafarkhani, H., [*Space-time coding: theory and practice*], Cambridge university press (2005).

[17] Tse, D. and Viswanath, P., [*Fundamentals of wireless communication*], Cambridge university press (2005).

[18] Bykhovsky, D., "Simple generation of gamma, gamma–gamma, and k distributions with exponential autocorrelation function," *Journal of Lightwave Technology* **34**(9), 2106–2110 (2016).

[19] Bykhovsky, D., "Comments on "simple generation of gamma, gamma–gamma and k distributions with exponential autocorrelation function"," *Journal of Lightwave Technology* **34**(14), 3411–3411 (2016).

[20] Hamkins, J., "Optimal codes for the burst erasure channel," *IPN Progress Report* , 42–174 (2008).

[21] Xu, F., Khalighi, M.-A., Caussé, P., and Bourennane, S., "Performance of coded time-diversity free-space optical links," in [*Proc. 24th Biennial Symposium on Communications*], 146–149, IEEE (2008).